

Bayesian reservoir characterization

Luiz Lucchesi Loures

ABSTRACT

This research aims to provide a complete solution for reservoir properties determination, including estimation and uncertainty analysis. The strengths of this reservoir characterization methodology is:

- i) uncertainty analysis and
- ii) integration of multiple geophysical data-sets, rock physics analysis and prior information in a straightforward way provided by the Bayesian framework.

The inference problem reported on this paper is formulated to solve the problem of porosity estimation. The sources of information are pre-stack seismic data; well log data and core samples. The reservoir is considered a volume composed of cells. The final solution is a probability density function (pdf) for porosity for each cell of the reservoir volume. These pdfs, call posterior pdfs, represent deductions about porosity and incorporate all related uncertainties.

The waveform elastic inversion is incorporated in this methodology to access the porous medium physical property information from pre-stack seismic data. Geostatistical modelling is incorporated to access the porous medium spatial variability information from well-log data.

The methodology is implemented to consider a reservoir composed for block cells. One posterior pdf is computed for each reservoir cell. Two cell volumes present the final result. One is constructed with the modes of the posterior pdfs related to each cell and represents the estimated porosity model, and the other is constructed with the confidence interval of the posteriors pdfs and represents a measure of the related uncertainties.

INTRODUCTION

Seismic attributes are the main source of information about the reservoir properties. In current reservoir characterization practices, seismic attributes are used together with well petrophysical measurements (from logs and core samples) to derive suitable calibrations of the rock physics and geostatistical models, which are key for reservoir quantification.

Despite the important decisions that are made after the reservoir quantification, the current reservoir characterization practices often fail to account for the uncertainties associated with each piece of information used in this process. Some uncertainty examples are related to: disturbances in the seismic data; data processing and inversion performed to obtain seismic attributes, the discrete earth model and the rock physics models relating attributes to petrophysical properties.

This work follows the Bayesian methodology of inference and provides a porosity estimated model and a related uncertainty analysis. The Bayesian methodology focuses

on obtaining a conditional probability density function (pdf) for the parameters under investigation, which is named the posterior pdf. This pdf comes from the normalized product of the prior pdf, constructed on the basis of information independent from the data, and the data pdf or likelihood function, which carries information from data fitting. In considering multiple datasets, we reinforce the idea that all data must be accounted for through a data fitting procedure. This yields a Bayesian formulation having multiple likelihood functions.

One of the main difficulties in the Bayesian formulation is working with high dimensional distributions. To avoid this problem, we use simple statistical models (e.g., Gaussian distributions) and the local distribution. In the local approach, we seek to directly obtain a collection of marginal posterior pdfs for individual parameters; e.g., interval porosity, in a 1-D inversion, or cell porosity in 2-D or 3-D inversions. Then all inferences, such as estimates or uncertainty measures, are taken from the marginal posterior pdfs.

This research report illustrates the principles of this formulation using the porosity inference example. The inference work is carried out on two levels, considering the different length scale of the datasets involved. On the first level there is the data obtained at well locations. Next, there is the inter-well space, where we must combine information propagated from the well location, surface seismic data, and rock physics analysis.

First a porosity inference at the well location is conducted from well-log data, following the work reported on Loures (2002). That work provides a posterior pdf of the interval porosity for each interval of a discrete well, which represents the beliefs about porosity given the knowledge of the well-log data.

The next problem concerns the porosity inferences at inter-well locations. Basically, the goal is to compute a marginal posterior distribution for the average porosity in each cell of the discrete reservoir model. In this case, we have divided the data information into two classes of data: one carrying information from the surface seismic data, which are the seismic attributes and another carrying information propagated from the well locations, which are the experimental variogram.

The waveform seismic inversion is incorporated into this Bayesian formulation via an elastic Bayesian inference work from pre-stack seismic data. This step follows the work of Gouveia and Scales (1998). The result of this inference work is a joint normal posterior pdf for the elastic parameters of a 1-D layered medium. Next, the parameters of these posterior pdf (i.e. the maximum a posteriori and the covariance matrix) together with rock physics models and petrophysic observations are the base for the likelihood function for the seismic attributes that represents the beliefs about porosity after the knowledge of the pre-stack seismic data.

Constructing a likelihood that carries information propagated from the well locations is a significant challenge. Defining the experimental variogram as the data to be inverted, and the variogram function as the mathematical expression relating this data to the cell porosity, solved it.

Finally, the porosity posterior pdf for a cell is the product of these pdf classes of likelihood, for the associated cell, and the prior pdf. This posterior pdf represents the

beliefs about the cell porosity given the knowledge of the pre-stack seismic data, which carry the porous medium elastic information, and the knowledge of well-log data, which carry the porous medium spatial variability information.

This report is going to describe the theoretical development, partial results of tests with pre-stack seismic data (1995 3-D Blackfoot data), practical implementation, a synthetic example and some discussion about the results and the further work.

BAYESIAN FORMULATION

Bayes Theorem

Consider the reservoir model composed by a set of N block cells with average porosity $\phi \in R^N$. The problem consists of making inferences about median porosity for each cell: $\phi_i, i=1, \dots, N$, using a set of data \mathbf{d} and prior information I , which is any additional information obtained independently from the data. Following the Bayesian approach of inference the solution is given by the posterior distribution $p(\phi | \mathbf{d}, I)$. This function is the result of the Bayes Theorem, which can be expressed as

$$p(\phi | \mathbf{d}) = \frac{l(\mathbf{d} | \phi) r(\phi | I)}{h(\mathbf{d} | I)}, \quad (1)$$

where $r(\phi | I)$ is the prior pdf, $l(\mathbf{d} | \phi)$ is the joint pdf for the data, also known as the likelihood function, and $h(\mathbf{d} | I)$ is a normalizing pdf that ensures the posterior distribution as a pdf. The posterior pdf should be expressed as the normalized product of prior distribution and likelihood function.

In order to consider the posterior pdf as the solution of an inverse problem, the likelihood must be defined (i.e. the relation between the data \mathbf{d} and the parameter ϕ exists and is known); and there are compatibilities between the prior understanding of the model and the final results, i.e. $l(\mathbf{d} | \phi) > 0$ for some ϕ where $r(\phi | I) > 0$. Now it is necessary to define the likelihood function and the prior distribution to access the posterior distribution.

Likelihood Function

This work follows standard steps to construct the likelihood function, which is summarized by:

- i)* selecting the datasets which carry information about ϕ ;
- ii)* finding mathematical expressions relating each type of porosity;
- iii)* defining statistical models (pdfs) for data distributions, based on data uncertainty.

Following these three steps, let us define the data set. This methodology defines two types of independent data set:

- i) a dataset of p-wave and s-wave velocity seismic attributes, represented by $\mathbf{s}=[\mathbf{s}_p, \mathbf{s}_s]^T$, $\mathbf{s} \in R^{2N}$ associated with the cells of the reservoir model and
- ii) a dataset carrying information about the spatial variability of reservoir porosity, which is represented by $\mathbf{v} \in R^L$.

Our choice is to make \mathbf{v} a set of experimental porosity-porosity variogram values computed from subsurface porosity information, after integration of multiple well-log datasets by a 1-D well-log porosity Bayesian inference procedure (for details please refer to Loures, 2002). That 1-D Bayesian well-log inference methodology provides a porosity model for a set of depth intervals at well locations and the associated uncertainty. That inference work shows that the integration of different types of well-log data provides a considerable reduction of systematic and random error components, which may occur when deriving porosity estimates from a single type of well-log data. The source of uncertainty is specific of each type of log.

Considering \mathbf{v} and \mathbf{s} as statistically independent datasets, the likelihood function should be expressed as the product of two independent distributions:

$$l(\mathbf{d} | \phi) = l(\mathbf{v}, \mathbf{s} | \phi) = l_1(\mathbf{v} | \phi) l_2(\mathbf{s} | \phi); \quad (2)$$

Data \mathbf{v} distribution: $l_1(\mathbf{v} | \phi)$

Assuming additive errors in the data \mathbf{v} , it should be written as

$$\mathbf{v} = \mathbf{f}_1(\phi) + \mathbf{e}_1, \quad (3)$$

where \mathbf{e}_i is a random variable representing a set of additive and independent errors. The error \mathbf{e}_i incorporates the uncertainties, which are associated with the porosity estimates in the well, the discrete earth model and the mathematical functions f_1 that relates these data with porosity.

The modelling operator f_1 is the variogram function from geostatistics. This function involves pairs of well-log porosity values ϕ and the unknown cell porosity, which is given by

$$\gamma(h) \equiv f_4(\phi) = \frac{1}{2NP} \sum_{i=1}^{NP} [\hat{\phi}(\mathbf{r}_i) - \phi(\mathbf{r}_i + \mathbf{h})]^2, \quad (4)$$

where \mathbf{r}_i and \mathbf{r}_{i+h} represent two different locations separated by a lag vector \mathbf{h} with dimension h and NP is the number of pairs.

Next step is to establish the criteria to select the probability density models for $l_1(\mathbf{v} | \phi)$ data pdf. We chose to use the principle of maximum entropy to assign probabilities and assume that the first and second order moment information is sufficient to describe the errors. According to these choices, the $l_1(\mathbf{v} | \phi)$ data pdf is normal and should be expressed as

$$l_1(\mathbf{v} | \phi, \sigma_1^2) = \frac{1}{2\pi\sigma_1^L} \exp\left\{-\frac{1}{2\sigma_1^2} [\mathbf{v} - \mathbf{f}_1(\phi)]^T [\mathbf{v} - \mathbf{f}_1(\phi)]\right\}, \quad (5)$$

and σ_1^2 considered the unknown data error variance. This choice criterion to construct a likelihood pdf will be used as a standard criterion elsewhere in this work.

Seismic data attributes distribution: $l_2(\mathbf{s} | \phi)$

Let \mathbf{s}_p and \mathbf{s}_s be a set of vectors representing p-wave and s-wave velocity seismic attributes respectively. These data vectors should be represented as the sum of a function of porosity, which are deterministic variables, and an error component, which is a probabilistic variable.

$$\begin{aligned} \mathbf{s}_p &= \mathbf{f}_2(\phi) + \mathbf{e}_2, \\ \mathbf{s}_s &= \mathbf{f}_3(\phi) + \mathbf{e}_3, \end{aligned} \quad (6)$$

The error \mathbf{e}_i , $i=2,3$ incorporate the uncertainties, which are associated with the process of data acquisition, data processing, the elastic inversion, the discrete earth model, and the mathematical functions \mathbf{f}_i , $i=1,2$ that relate these data with porosity.

The next step is to define the relationships between data vectors and porosity, represented by the functions $\mathbf{f}_1(\phi)$ and $\mathbf{f}_2(\phi)$. The choice is the rock physics models studied by Han *et al* (1986).

$$\mathbf{f}_2(\phi) = a_2 + b_2\phi + c_2\gamma; \quad (7)$$

$$\mathbf{f}_3(\phi) = a_3 + b_3\phi + c_3\gamma; \quad (8)$$

where γ is the unknown clay content and a_i , b_i and c_i for $i=1,2$ are the unknown regression coefficients. The set of equations (6), after the substituting equations (7) and (8), should be treated as multi-regression model with auto-correlated errors (Zelner and Tiao, 1964). In rock physics and elsewhere we encounter sets of regression equations and it is often the case that the disturbances are correlated. It is important that non-independence of disturbances terms be taken into account in making inferences. If this is not done, inferences may be greatly affected.

The $l_2(\mathbf{s} | \phi)$ pdf is defined as a normal distribution, as previously done for $l_1(\mathbf{v} | \phi)$, but two statements are considered to construct this pdf:

- i)* These rock physics models do not consider explicitly some petrophysical properties that strongly affect the seismic velocities (for example fluid properties and effective pressure). The unknown regression coefficients incorporate the effect of these petrophysical properties. The likelihood pdf $l_2(\mathbf{s} | \phi)$ must to incorporate the rock physics associated uncertainty.
- ii)* The seismic elastic attributes come from a elastic inversion. A mutual correlation between the attributes exists, i.e. the random variables \mathbf{e}_1 and \mathbf{e}_2 are

not mutually independent. Its posterior covariance has a nonzero off-diagonal covariance matrix;

To consider the first statement, this work uses a property of the Bayesian inference to predict a pdf for a new observation given an old observation. For the second statement this work uses a seismic elastic inference that provide an elastic model for layered medium and the associated covariance matrix. The next sections describe the theory of this Bayesian property applied to this current problem.

The predictive pdf

The predictive pdf for a vector of future observation \mathbf{s} , which is assumed to be generated by the multiple regression process specified by the set of equations (6), is derived after the knowledge of an old set of observations \mathbf{s}^* , which is assumed to have the same statistical properties of \mathbf{s} .

For this present inference problem, consider a reservoir section composed by cells represented by the image in Figure 1. The vertical axis is the depth and the horizontal axis is the horizontal distance. The vertical lines represent well positions. Consider an available set of seismic attributes related to the reservoir cells.

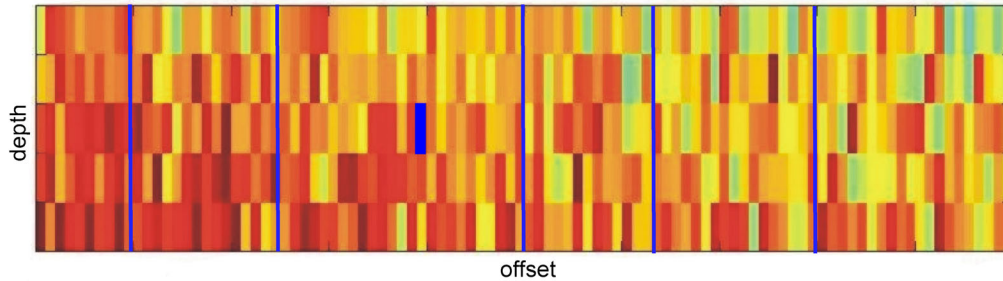


FIG 1: This image represents a reservoir section composed by block cells. The vertical axis is the depth and the horizontal axis is the horizontal distance. The vertical lines represent well positions.

Let's consider $\mathbf{s}^* = [\mathbf{s}_p^* \ \mathbf{s}_s^*]$ the seismic attributes estimated for the cells at well locations. \mathbf{s}_p^* and \mathbf{s}_s^* represent a vector of the p-wave and s-wave velocities respectively for the cells at the well locations. A multiple regression process with the set of equations (6) can generate the vector \mathbf{s}^* , where the regression coefficients are unknown variables and the petrophysical properties porosity ϕ and clay content γ , which represent the control variables, are known from well-log petrophysical observations. This set of equations can be represented in vector form as:

$$\mathbf{s}^* = \mathbf{X}\mathbf{P} + \mathbf{e}^* ; \tag{9}$$

where \mathbf{X} is a matrix composed by a unit vector column and with the petrophysical observations (from logs and core samples analysis) along the well;

$\mathbf{P} = \begin{bmatrix} a_1 & a_2 \\ b_1 & b_2 \\ c_1 & c_2 \end{bmatrix}$ is a matrix with the unknown regression coefficients and \mathbf{e}^* is the

disturbance term normal distributed, with mean zero and known covariance matrix.

The posterior pdf for these unknown regression coefficients can be found applying the Bayesian theorem. Considering a non-informative prior distribution (for detail, please refer to Zellner, 1998) the posterior pdf for the regression coefficients should be represented by

$$p(\mathbf{P} | \mathbf{s}^*, \mathbf{X}) \propto \exp\left\{-\frac{1}{2}[(\mathbf{s}^* - \mathbf{XP})^T \mathbf{C}_{s^*}^{-1}(\mathbf{s}^* - \mathbf{XP})]\right\}; \quad (10)$$

where \mathbf{C}_{s^*} is the covariance matrix of the seismic attributes.

Now, let's consider the seismic attributes from a cell at inter-well space $\mathbf{s} = [s_p \ s_s]$, for example, the blue cell in the reservoir section of Figure 1. s_p and s_s are respectively the p-wave and s-wave velocity seismic attributes obtained for this specific cell. At this position the petrophysical information about porosity and clay content are not available. Representing this multiple regression process by a vector equation results in

$$\mathbf{s} = \mathbf{w}^T \mathbf{p} + \mathbf{e} \quad ; \quad (11)$$

where $\mathbf{w}^T = [1 \ \phi \ \gamma]$, is a vector with the unknown petrophysical properties of the associated cell, \mathbf{e} is disturbance term normal distributed and with median zero and the same statistical properties of \mathbf{e}^* .

One way of deriving the predictive pdf is to write down the joint pdf $l^+(\mathbf{s}, \mathbf{P} | \mathbf{S}^*, \mathbf{X}, \mathbf{w})$ and integrate with respect to \mathbf{P} to obtain the marginal pdf for \mathbf{s} , which is the predictive pdf. In the present problem this joint factors as follows:

$$l^+(\mathbf{s}, \mathbf{P} | \mathbf{S}^*, \mathbf{X}, \mathbf{w}) = l^*(\mathbf{s} | \mathbf{P}, \mathbf{w}) p(\mathbf{P} | \mathbf{S}^*, \mathbf{X}) \quad (12)$$

Substituting Equation (10) with Equation (12) and developing $l^*(\mathbf{s} | \mathbf{P}, \mathbf{w})$ the following expression is found:

$$l^+(\mathbf{s}, \mathbf{P} | \mathbf{S}^*, \mathbf{X}, \mathbf{w}) = \exp\left\{-\frac{1}{2}[(\mathbf{s} - \mathbf{w}^T \mathbf{P})^T \mathbf{C}_d^{-1}(\mathbf{s} - \mathbf{w}^T \mathbf{P}) + (\mathbf{S} - \mathbf{XP})^T \mathbf{C}_d^{-1}(\mathbf{S} - \mathbf{XP})]\right\} \quad (13)$$

This final joint pdf represents the data distribution for the seismic attributes of a specific cell at inter-well space and incorporates the rock physics knowledge from well petrophysic observations (core samples and logs).

Prior distribution

This work considers the definition of a non-data base prior distribution (NDBP) described by Jeffreys (1936) to access the prior distribution. A NDBP is derived from

theoretical knowledge of the physical medium and from the investigator's background experiences.

In this work the prior distribution must describe the prior knowledge of the unknown experimental variogram data variance and porosity.

This report follows the Bayesians' most conservative practice to define the prior pdf. It considers that with all previous pieces of information available, the only verifiable statement is that porosity should fall between 0 and 1 interval. The use of a boxcar function is consistent with expressing this prior information (for more details please refer to Zellner, 1996)

The prior experimental variogram data-variance knowledge is that these scaling parameters may vary between 0 and ∞ . Following Jeffreys (1939) the use of an improper distribution is consistent to express complete unawareness of such parameters (i.e. any value between 0 and ∞ is equiprobable). Its logarithm pdf should be deemed as uniformly distributed and the use of a $r(\sigma_1) \propto 1/\sigma_1$ function is considered a reasonable choice in describing this information. This pdf is invariant under power transformation. Then, prior distribution should be expressed as

$$r(\phi, \sigma_1 | I) \propto \frac{1}{\sigma_1}, 0 \leq \phi \leq 1 \quad (14)$$

Note that the prior pdf is improper, i.e. it is not normalized

Posterior distribution

With the Bayes Theorem applied, the posterior distribution should be

$$p(\mathbf{w}, \sigma_1^2, \mathbf{P} | \mathbf{v}, \mathbf{s}, \mathbf{S}^*, \mathbf{X}) \propto l_1(\mathbf{v} | \phi, \sigma_1^2) l_2(\mathbf{s}, \mathbf{P} | \mathbf{S}^*, \mathbf{X}, \mathbf{w}) r(\phi, \sigma_1 | I) \quad (15)$$

The experimental variogram data variances σ_1^2 and the regression coefficients (on vector \mathbf{P}) are not the target of investigation. Petrophysical property inference and associated uncertainty is all that matters in this problem. These uninteresting parameters, which are referred to as nuisance parameters, are eliminated by integration of the joint posterior. This procedure, which is known in statistics as marginalization of the joint distribution, is applied and the marginal posterior pdf is obtained:

$$p(\mathbf{w} | \mathbf{v}, \mathbf{s}, \mathbf{S}^*, \mathbf{X}) \propto \iint p(\mathbf{w}, \sigma_1^2, \mathbf{P} | \mathbf{v}, \mathbf{s}, \mathbf{S}^*, \mathbf{X}) d\sigma_1^2 d\mathbf{P} \quad (16)$$

This final pdf represents the data distribution for \mathbf{w} of a cell at the inter-well space and incorporate the knowledge from petrophysical wells observations and from surface seismic data.

All inference questions can be addressed to the posterior. For example, one can use the mean, median or mode as estimates for the interval porosity and the standard deviation or confidence intervals as measure of uncertainty.

A 1-D example of the application of this methodology from a cdp gather is presented at the next section.

1-D EXAMPLE

The seismic elastic inference: a full waveform inversion

The first step in this methodology is a seismic elastic inference, which provides an elastic model of the medium and the associated covariance matrix. This work follows the methodology presented by Gouveia and Scales (1998), who developed a Bayesian formulation for the pre-stack seismic inverse problem, to estimate elastic velocities and density or elastic impedances. In their work, all uncertainties are described by normal distributions, but careful consideration is taken to construct the covariance matrices. These matrices are responsible for expressing all uncertainties in a normal pdf.

This methodology considers a 1D reservoir with n-layers. The layers' thicknesses do not vary during the inversion process. Elastic velocities (P and S-wave velocities) and densities from layers of a target interval are inverted from a CDP gather.

According to the Bayes' Theorem the general formulation of this seismic inverse problem, can be written as

$$p(\mathbf{s} | \mathbf{d}, I) \propto l(\mathbf{d} | \mathbf{s}) r(\mathbf{s} | I) \quad (17)$$

where $p(\mathbf{s} | \mathbf{d}, I)$ is the resulting posterior pdf for the seismic attributes and $l(\mathbf{d} | \mathbf{s})$ and $r(\mathbf{s} | I)$ are, respectively, the likelihood and the prior pdf. \mathbf{s} represents the elastic attributes and \mathbf{d} the pre-stack seismic data.

In defining the probability models, one problem arises due to the non-linearity of the forward seismic problem $\mathbf{d} = \mathbf{g}(\mathbf{s})$, where the \mathbf{g} is the seismic modelling operator defined by the elastic reflectivity method (Muller, 1985). Even when the prior pdf and likelihood are Gaussian, the posterior pdf $p(\mathbf{s} | \mathbf{d})$ cannot be obtained in closed form. Only in the case that the forward problem is linear, is $p(\mathbf{s} | \mathbf{d})$ Gaussian.

The standard solution is to first to obtain optimum estimates for the elastic properties $\hat{\mathbf{s}}$, then a Gaussian approximation for $p(\mathbf{s} | \mathbf{d})$ is constructed on the basis of the linearization of the forward problem around point $\hat{\mathbf{s}}$. This optimization process is designed on the basis of Equation (17) to yield the point of maximum probability density. When $l(\mathbf{d} | \mathbf{s})$ and $r(\mathbf{s} | I)$ are both Gaussian, maximizing probability density is equivalent to minimizing the exponential argument of the Gaussian, leading to standard non-linear least square problem. Again, assuming diffuse or non-informative prior information, which makes

$$p(\mathbf{s} | \mathbf{d}) \propto l(\mathbf{d} | \mathbf{s}) \quad (18)$$

and the argument of the exponential of the likelihood

$$\mathbf{arg}(\mathbf{s}) = [\mathbf{d} - \mathbf{g}(\mathbf{s})]^T \mathbf{C}_d^{-1} [\mathbf{d} - \mathbf{g}(\mathbf{s})] \quad (19)$$

where \mathbf{C}_d is the seismic data covariance matrix.

The process of optimization by conjugate gradient used in Gouveia and Scales (1998), and adapted by the purpose of this work, can be summarized by the following expression:

$$\mathbf{s}_{n+1} = \mathbf{s}_n + \eta \delta_n \quad (20)$$

where δ_n is the direction of the n th iteration step and η is the step length. The gradient of the function represented by Equation (19) is given by

$$\nabla \Theta = \mathbf{G}(\mathbf{s}) \mathbf{C}_d^{-1} (\mathbf{d} - \mathbf{g}(\mathbf{s})) \quad (21)$$

where $\mathbf{G}(\mathbf{s})$ is the matrix of Fréchet derivatives of the forward term $\mathbf{g}(\mathbf{s})$. After completing the optimization process, the resulting Gaussian approximation for the seismic attributes around \mathbf{s} can be expressed by

$$p(\mathbf{s} | \mathbf{d}) \propto \exp \left\{ -\frac{1}{2} [\mathbf{s} - \hat{\mathbf{s}}]^T \mathbf{C}_s^{-1} [\mathbf{s} - \hat{\mathbf{s}}] \right\}, \quad (22)$$

where the covariance matrix is $\mathbf{C}_s = [\mathbf{G}^T \mathbf{C}_d^{-1} \mathbf{G}]^{-1}$ which the Fréchet derivatives evaluated at $\hat{\mathbf{s}}$.

A vertical component cdp gather from the 1995 Blackfoot dataset, adjacent to the well 0808, was selected for this 1-D example. The Blackfoot area is located 15 km southeast of Strathmore, Alberta, Canada. The target rocks are incised valley-fill sediments, which consists of the lower Cretaceous sandstone of Glauconitic Formation at the Blackfoot Field. In the Blackfoot area the Glauconitic sands thickness varies from 0 to over 35 m. It is subdivided into three phases of valley incision that, however, cannot be found everywhere. The lower and upper members are made of quartz sandstone, 0.18 porosity average, while the middle member consists of low porosity tight lithic sandstone.

A previous processing in this 3D dataset has the following steps:

- i) mute;
- ii) all static corrections;
- iii) surface consistent deconvolution;
- iv) true amplitude recovery;
- v) band-pass

Figure 2 shows the selected cdp gather. The target interval is between 1.0 s and 1.1 s (1510-1710 m) and represents the Mannville Formation. This interval is discretized in 10 m layers. The Figure 3 shows the elastic model obtained by the maximum a posteriori,

together with the well logs from the well 0808 and the initial model for the iteration process. The initial model is obtained from the sonics and density logs (from well 0808) after applied moving window of 200 m and blocked to 10 m. The final result shows a considerable improvement of the estimates regarding the initial model. The Glauconitic channels are present in the base of this interval, between 1.665 m and 1710 m.

Figure 4 is an image representing the covariance matrix, with colour scale where red is high value and green is low value. We can note the correlation between the elastic attributes in the off diagonal of the covariance matrix (the gradual variations of the off diagonal elements of this covariance matrix are not clear enough in a black and white hard copy).

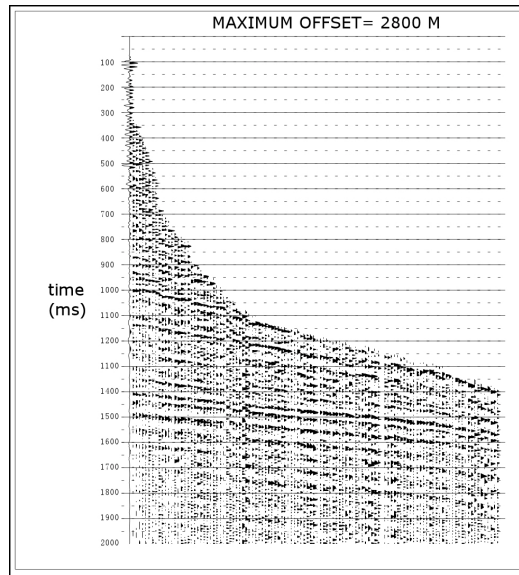


FIG 3: cdp gather close the well log 0808 at Blackfoot area, selected for a 1-D example. The target interval is between 1s and 1.1 s (1510-1710 m).

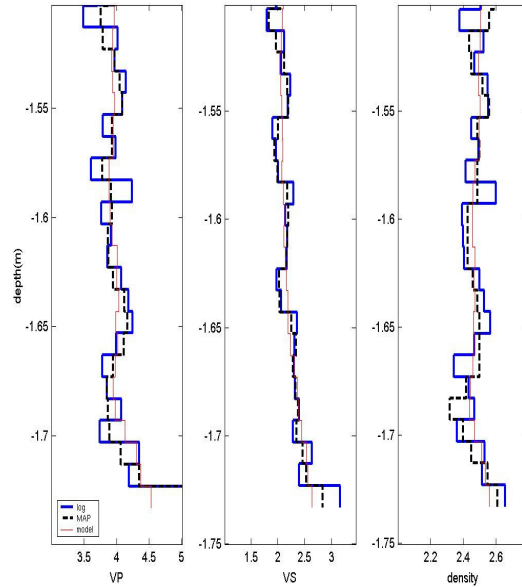


FIG 4: Elastic velocities and density obtained by the maximum a posteriori (black line curves or black continuous light in black and write copy), together with the well logs (sonics and density logs) from the well 0808 (blue line curves or light continuous line in black and write copy) and the first model for the iteration process (red line curves or dashed line in black and write copy).

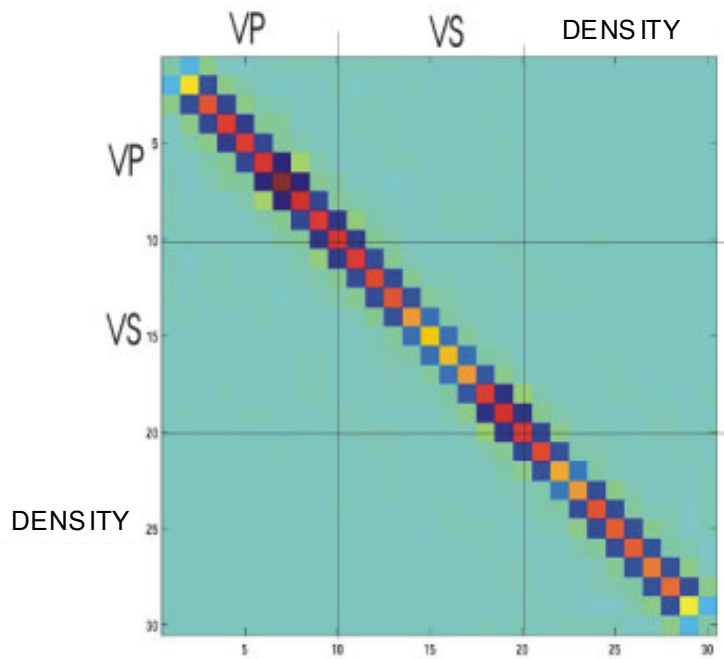


FIG 5: The posterior covariance matrix for the seismic attributes (elastic velocities and density), with a colour scale where red is high value and green is low value (the slowly variations of the off-diagonal elements of this covariance matrix are not clear in black and white).

The petrophysical inference

A 1D porosity inference is applied on the interval of the Glauconitic Sandstone reservoir channels in the well 0808 (between 1.665 m and 1710 m) using the Equation (16) and the results of the previous elastic inference. In this example the clay content is considered a known parameter ($\gamma = \gamma_0$). This information comes from gamma ray log. Then the posterior distribution for porosity, expressed by Equation (16), can be rewritten as $p(\phi | \mathbf{s}, \mathbf{s}^*, \mathbf{X}, \gamma = \gamma_0)$.

The well 1608, from Blackfoot area, is used to construct the matrix \mathbf{X} and \mathbf{s}^* needed in the posterior pdf. Porosity estimates from core laboratory analysis and clay content estimates from gamma ray log are used to construct the matrix \mathbf{X} . Seismic attribute estimates from a cdp gather adjacent the well 1608 are used to construct the matrix \mathbf{s}^* . Figure 6 illustrates the position of the well 1608 and the well 0808 used in the Blackfoot area.

A posterior pdf $p(\phi | \mathbf{s}, \mathbf{s}^*, \mathbf{X}, \gamma = \gamma_0)$ is computed for each 10 m interval of the glauconitic channels. The final result is a collection of posterior pdfs representing one posterior pdfs for each 10 m layer. Figure 7 illustrates the results from three different porosity inversions using different amounts of seismic information. These are respectively a test using only p-wave elastic velocity, a test using only s-wave elastic velocity and using both p and s-wave velocities, resulting the following posterior pdfs: $p(\phi | \mathbf{s}_p, \mathbf{S}^*, \mathbf{X}, \gamma = \gamma_0)$, $p(\phi | \mathbf{s}_s, \mathbf{S}^*, \mathbf{X}, \gamma = \gamma_0)$ and $p(\phi | \mathbf{s}, \mathbf{S}^*, \mathbf{X}, \gamma = \gamma_0)$. Such posterior pdfs are presented by images with a colour scale. The vertical axis of these images represents the depth and the horizontal axis represents porosity values and the colour scale represents the probability amplitudes of the posteriors pdfs. The black line in the images represents the porosity model from core laboratory analysis. We can see from the spread of the posterior pdfs that the inversion of p-wave velocity has lower resolution than the when s-wave velocity. When both velocities are used together it has higher resolution.

From analyses of these images together with the core sample porosity estimates one may conclude that the 10 m layer 1-D model does not have sufficient resolution to describe the sandstone channels. A thinner layer model is necessary to describe the channels. This is a limitation of the vertical seismic resolution. It is a typical example of the ill-posed inverse problem.

The seismic inversion is still the main challenge in this methodology. Resolution of the seismic inversion is currently being improved in two ways:

- i) pre-stack time migration has been carried out to enhance the signal to noise ratio;
- ii) an investigation is underway to evaluate the practicality of introducing prior information from a high-resolution seismic stratigraphic interpretation via regularization.

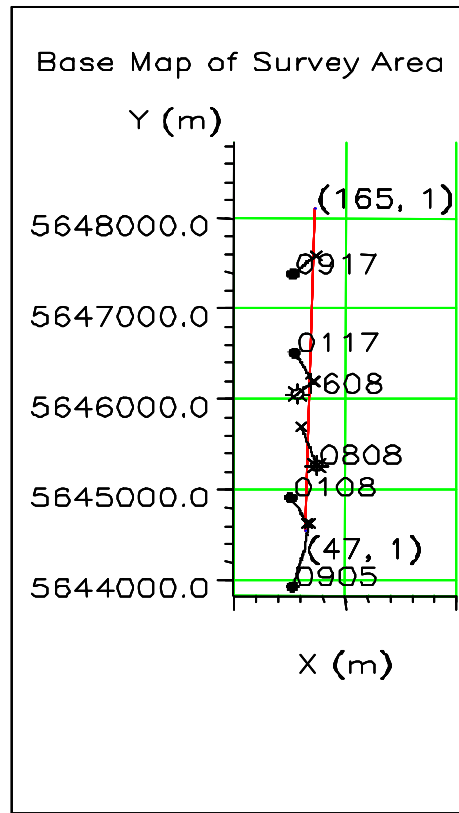


FIG 6: The base map of the area with the position of some well logs.

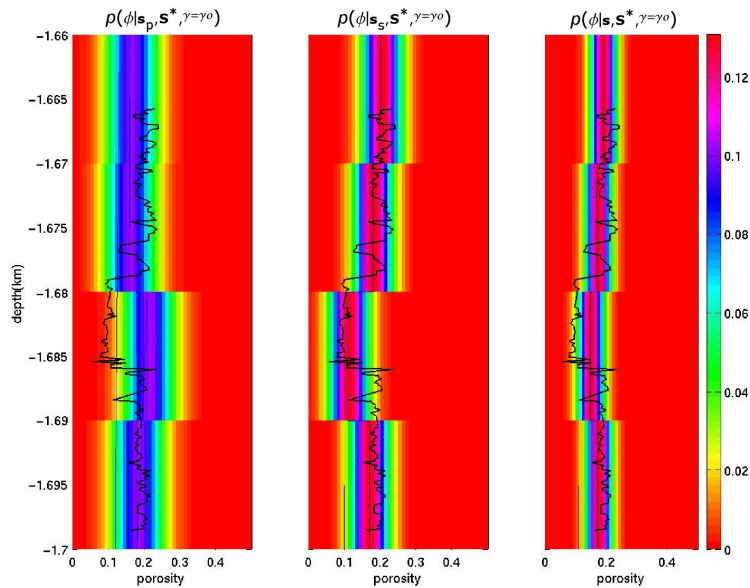


FIG 7: These images represent the posterior pdfs for three different tests: using only p-wave velocity (left), using only s-wave velocity (centre) using both p and s-wave velocities (right). The vertical axis represents the depth and the vertical axis the porosity values. The colour bar scale represents the probability amplitude and the black line the porosity from laboratory analysis from core sample of the well 0808.

PRACTICAL IMPLEMENTATION

Using a horizontal moving window, running across the reservoir volume (3-D) or a reservoir section (2-D), a distribution $l_2(\mathbf{s}|\phi) = l(\mathbf{s}, \mathbf{P} | \mathbf{S}^*, \mathbf{X}, \mathbf{w})$ is calculated for a cell in the centre position of each window (the data vector \mathbf{s} is the seismic attributes from cells falling inside the window). The Fresnel Zone can be considered for defining the dimension of the window, allowing it to vary across the reservoir. In the same way, $l_1(\mathbf{v}|\phi)$ is also computed for each cell position. Finally, both distributions are combined by the application of Equation (15) to yield one posterior pdf for each cell of the reservoir.

Two volumes of the discretized reservoir represent the final results. One shows the mode of the posterior pdfs, representing the final estimated porosity model, and another shows the length of 0.95 posterior probability centred at the mode, representing the associated uncertainty model.

Synthetic data example is presented to show how this methodology works. Three different tests are performed to evaluate the importance of each set of data \mathbf{v} and \mathbf{s} in increasing the confidence of porosity estimates: using only dataset \mathbf{s} , which gives the posterior $p(\phi|\mathbf{s}) \propto l_2(\mathbf{s} | \mathbf{X}, \mathbf{s}^*, \phi)q(\phi)$, using only the data set \mathbf{v} , which gives $p(\phi|\mathbf{v}) \propto l_1(\mathbf{v}|\phi)q(\phi)$, and using both datasets ($p(\phi|\mathbf{v}, \mathbf{s}) \propto l(\mathbf{v}, \mathbf{s} | \mathbf{X}, \mathbf{s}^*, \phi)q(\phi)$).

SYNTHETIC DATA EXAMPLE

Using a 2-D model of vertical and lateral changes in porosity (Figure 8) the seismic attributes p and s -wave velocities and density and the well logs: neutron porosity, compression and shear sonics velocities, density and gamma ray logs are simulated. The gamma ray log is used to obtain information about clay content of the medium. The clay content γ of this model is constant and equal 0.5 and the effective pressure is assumed 0.4 kbar/cm³.

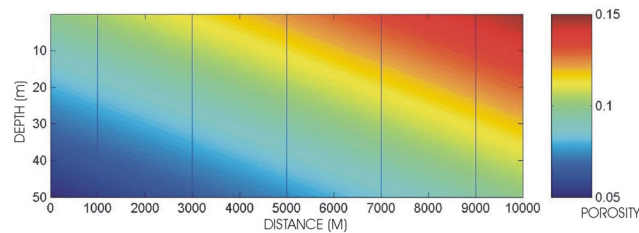


FIG 8. Image representing the true porosity model used in the synthetic data example. Vertical lines show the locations of 5 wells distributed across the model. The colour bar scale represents the porosity.

All simulated well log data are corrupted with pseudo-random gaussian noise with zero mean. Additionally, a systematic error component of 10 % is included in the neutron porosity log. The noise-corrupted logs, from the log at 1000 m distance in the Figure 8, are shown in Figure 9.

The seismic attributes are simulated for the model of Figure 8. The standard deviation of the noise is defined based on examples of elastic inversion available at literature (e.g.,

Debski and Tarantola (1995)), respectively 10 %; 20 % and 30 % for p-wave velocity, s-wave velocity and density respectively.

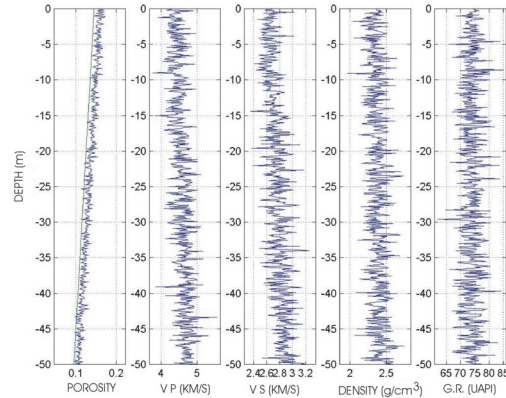


FIG 9: Synthetic well log data for the first well (1000 m distance) represented in the model of Figure 8. These are, from left to right, neutron porosity, sonic logs (compression and shear wave velocities), density and gamma ray. All log data are corrupted with pseudo random Gaussian noise. In addition, the porosity neutron log has a shift of 10 % of the true porosity model to simulate a calibration error. The green line in the porosity log plot represents the true porosity.

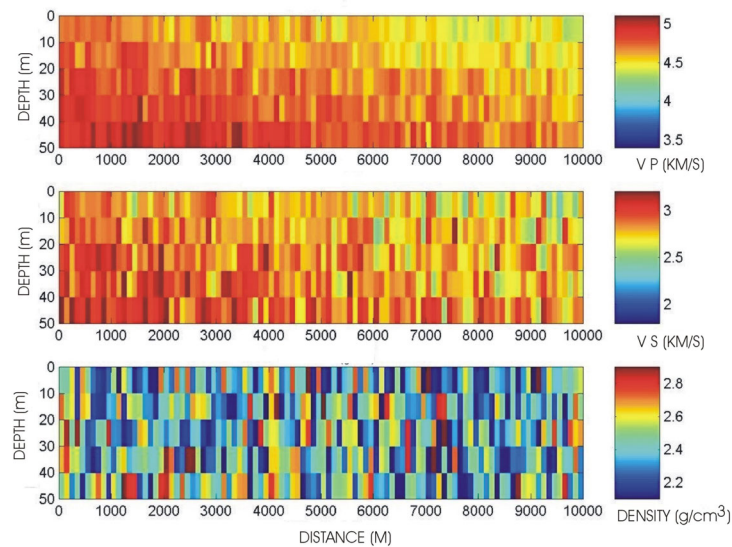


Figure 10: Seismic attributes p-wave velocity, s-wave velocity and density, respectively the images from top, middle and bottom calculated from the geologic model (Figure 8) and corrupted with pseudo-random Gaussian noise with mean zero.

As described above, the first step in the application of the proposed methodology is to precede the inversion of well-log data. These well-log inversions follow Loures (2002). Figure 11 shows the resulting porosity pdfs for each depth interval along the wells. The modes of these pdfs are estimates for interval porosity at the wells. Data vector v is

generated from the well porosities estimates using experimental horizontal variogram calculated with a lag spacing of 2 km.

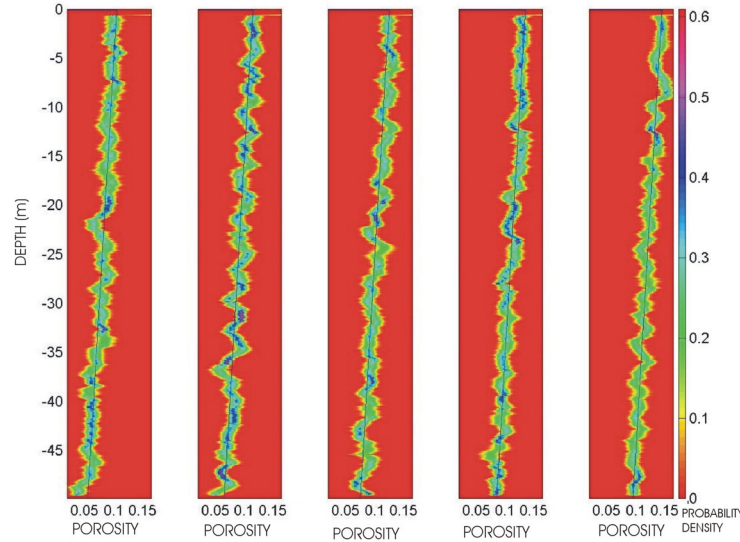


Figure 11: Images representing the distributions for interval porosity for each well from the model (Figure 8), as the results of the application of the inversion procedure by Loures (2002). For a fixed depth interval, the colour scale gives the posterior pdf for porosity. Porosity estimates are taken from the mode of the posterior at each depth interval. The spread of the distribution around the mode gives an idea of the associated uncertainty.

The next step is the evaluation of both functions $l_1(\mathbf{v}|\phi)$ and $l_2(\mathbf{s}|\mathbf{X}, \mathbf{s}^*, \phi)$ for each cell to compute the posterior pdfs as their product. To do that, an interpretative model composed of cells 100 m wide by 10 m thick is used. A moving 2-D window, covering three cells (10 x 300 m), is used to obtain the likelihood in each cell of the reservoir. As explained before, to evaluate the individual contributions of well information and seismic attributes data, the posterior distribution is computed using three different data combinations: using well and attribute data individually ($p(\phi|\mathbf{s})$ and $p(\phi|\mathbf{v})$) and both datasets combined ($p(\phi|\mathbf{v}, \mathbf{s})$).

To compute $l_2(\mathbf{s}|\mathbf{X}, \mathbf{s}^*, \phi)$ the clay content γ is considered an a priori known parameter. These parameters are estimated for the cells at inter well space using the clay content estimation from the gamma ray log and a variographic modelling.

The porosity models obtained by the mode of posterior distributions are shown in Figure 12. At the top, Figure 12A, one can find the result obtained just from the use of variogram data (\mathbf{v}). The middle Figure 12B shows the result obtained just from the use of seismic attribute data (\mathbf{s}). Finally, the bottom Figure 12C shows the result of using both data types (\mathbf{v} and \mathbf{s}). Reasonable models of porosity are obtained. The model shown by Figure 12A has a horizontal variation pattern characterized by step variations. The positions of these steps are related to the lag limits and well positions. The model shown by Figure 12B has high frequency horizontal variations derived from the random noise in

the seismic attribute data. The Figure 12C shows a porosity model that has a more slowly varying porosity than the model from Figure 12A and no high frequency variations around the well position, where the data v has more influence on the estimates.

Figure 13 shows the length of the centred interval having 0.95 probabilities, corresponding to each one of the estimates in Figure 12. This gives a measure of the spread of the posterior pdf and the resolution for porosity of each cell of the reservoir. Figure 13A shows that the data v is more informative for cells near the well than for cells further away. Figure 13B shows that the information about porosity contained in the seismic attributes is homogeneously distributed across the section, yielding high-frequency variations on the estimates. Figure 13C shows us an improvement of the resolution of a model when the porosity information from both well-log and seismic attributes data are integrated by the bayesian formulation.

CONCLUSION

The methodology presented is an approach to reservoir characterization fully grounded on the inversion theory, which is capable integrating multiple datasets in a straightforward way. The commonly employed formulations of the mathematical physics relating data and model parameters are replaced by empirical formulas of experimental rock physics. Geostatistics is also integrated through the experimental variogram and the corresponding formula, both used in the context of inversion theory. A synthetic data test using a slowly varying model demonstrated the consistency of the proposed methodology.

The pre-stack seismic information is accessed via an elastic inversion. The real 1-D example shows that the elastic inversion is still the main challenge in this work. The main limitation is the vertical resolution of the model.

Analysis of results of the synthetic 2-D example shows reasonable reconstructions of the true porosity model obtained from the mode of the posterior pdfs. The associated uncertainty, represented by the length of 0.95 probability intervals, consistently varies depending on the amount of information available. Higher resolution is obtained at the wells. The variogram fitting procedure allowed describing the information about the porosity from the wells at inter-well locations. For the inversion of seismic attributes alone the level of uncertainty varies homogeneously across the model. When combining variogram and attribute data, we observe that the overall uncertainty is reduced and the porosity model is better reconstructed.

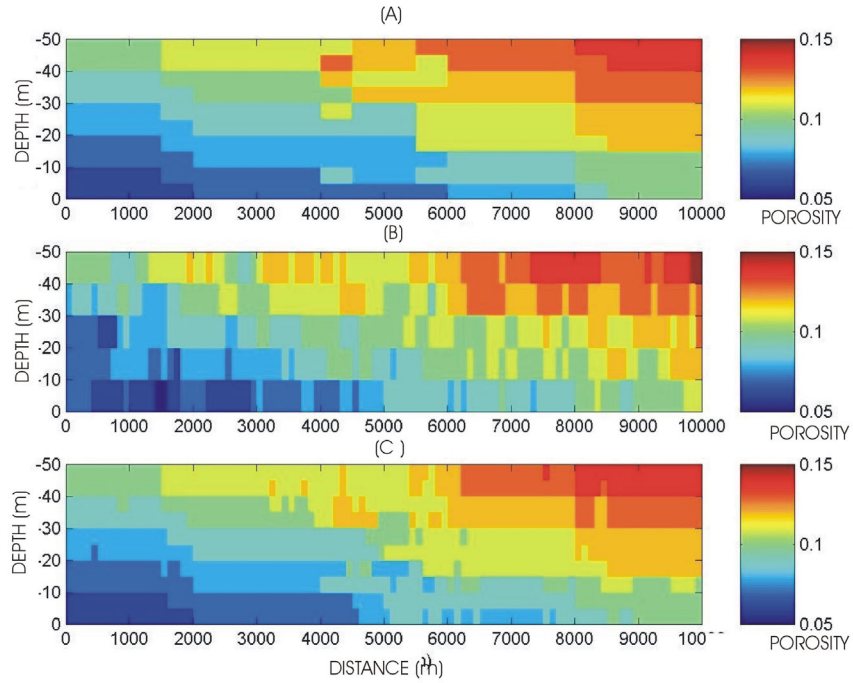


FIG 12: Images of the reservoir section representing the modes of the posterior distributions by the use of variogram data (A), seismic attributes (B) and both datasets (C).

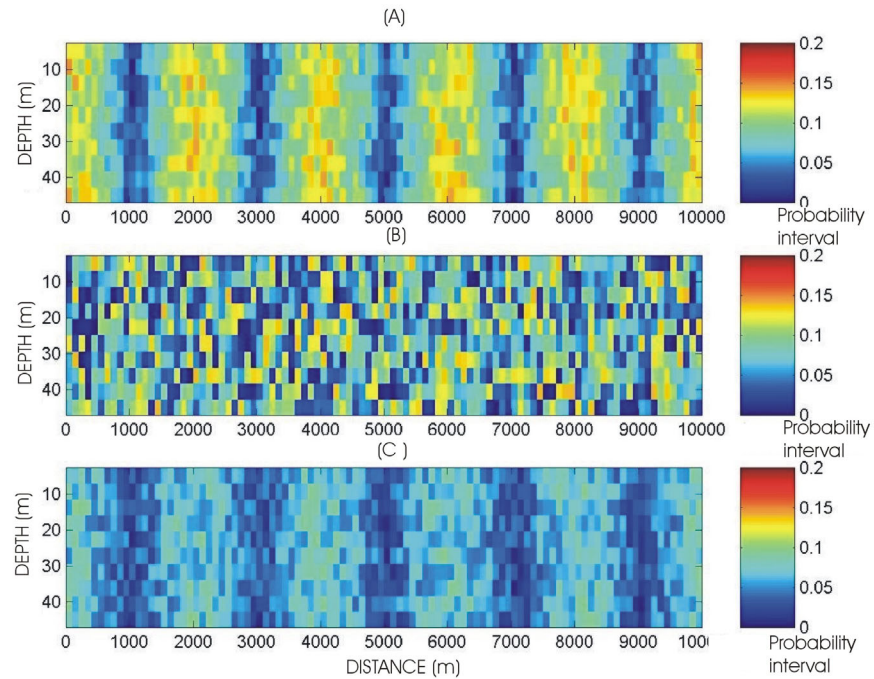


FIG 13: Images of the reservoir section representing the length of the 0.95 probability interval of the posterior distributions obtained from the inversion of variogram values (A), seismic attributes data (B) and both datasets (C).

FUTURE WORK

1. The application of the proposed methodology to 3D-3C Blackfoot seismic data (1995).
2. An investigation of extensions of this methodology to infer other petrophysical properties has been started. The evaluation of the viability of using other rock physics models to fluid property and permeability inferences has been started with a new Bayesian formulation.
3. Implementations of the seismic elastic inference work to incorporate prior information from seismic stratigraphic interpretations and investigation of the use of the radial component in this process.

ACKNOWLEDGEMENTS

We wish to thank the sponsors of CREWES, to CNPq; a Brazilian Federal Agency for scientific and technological development. We would like to thank Wence P. Gouveia and the members of CREWES, specially for Han-xing Lu for help with data processing and discussions in reflectivity modelling, for the Professors Gary Margrave and Larry Lines, researcher, Charles Ursenbach, and the PhD student, Jonathan Downton, for helpful discussions.

REFERENCES

- Duijndam, A.J.W., 1988, Bayesian estimation in seismic inversion. Part I: Principles. *Geophys. Prosp.* , **36**, 878-898.
- Debski, W. and Tarantola, A., 1995, Information on elastic parameters obtained from the amplitudes of reflected waves. *Geophysics* **60**, 1426-1436.
- Eberhart-Philips, D., Han, D., and Zoback, M.D., 1989. Empirical relationships among seismic velocity, effective pressure, porosity and clay content in sandstone. *Geophysics*, **54**, 82-89.
- Gouveia, W. and Scales, J.A., 1998, Bayesian seismic waveform inversion: Parameter estimation and uncertainty analysis, *J. Geophys. Res.*, **103**, 2759-2779.
- Jeffreys, H., 1936, *Theory of Probability*: Oxford University Press, London.
- Han, D.H., Nur, A., and Morgan, D., 1986, Effects of porosity and clay content in wave velocities in sandstones. *Geophysics*, **51**, 2093 – 2107.
- Loures, L., 2002, Porosity inference from multiple well log data, CREWES Research Report, Vol. **14**
- Muller, G., 1985, The reflectivity method: a tutorial: *Journal of Geophysics*, **58**, 153-174.
- Zellner, A., 1996. *An Introduction to Bayesian Inference to Econometrics*, Willey Intercience.
- Zellner, A. and Tiao, G.C., 1964, Bayesian analysis of the regression model with autocorrelated errors, *J. Am. Statist. Assoc.*, **59**, 763-778.